The X-ray structure of photosystem II reveals a novel electron transport pathway between P680, cytochrome b_{559} and the energy-quenching cation, Chl_Z^+

Sergej Vasil'ev[a], Gary W. Brudvig[b], Doug Bruce[a,*]

[a] *Department of Biological Sciences, Brock University, St. Catharines, ON, Canada L2S 3A1*
[b] *Department of Chemistry, Yale University, P.O. Box 208107, New Haven, CT 06520-8107, USA*

Received 13 March 2003; revised 7 April 2003; accepted 8 April 2003

First published online 1 May 2003

Edited by Richard Cogdell

Abstract When water oxidation by photosystem II (PSII) is impaired, an oxidized chlorophyll (Chl_Z^+) is formed that quenches excitation and may prevent photodamage. Both the identification of this Chl^+ and the mechanism of its oxidation and reduction are controversial. Using the available X-ray structures of PSII we calculated the efficiency of two proposed quenchers, Chl_Z^+(D1) and Chl_Z^+(D2). Of these two, only Chl_Z^+(D1) can quench to the degree observed experimentally. We also identify a chain of closely spaced pigments in the structure from *Thermosynechococcus vulcanus* that we propose to form a novel electron transport pathway between Chl_Z(D1), β-carotene, $P680^+$ and cytochrome b_{559}.

Key words: Photosynthesis; Non-photochemical quenching; Chlorophyll fluorescence; Excitation energy transfer; Electron transport

1. Introduction

Photosystem II (PSII) captures the energy of sunlight and catalyzes the oxidation of water and reduction of plastoquinone in photosynthetic electron transport. These reactions involve a dangerous stepwise accumulation of redox potential that sensitizes PSII to photoinduced damage. PSII exhibits a number of mechanisms that serve either a protective or a repair role in response to such light-induced damage [1].

The reaction center (RC) of PSII consists of the D1 and D2 polypeptides, cytochrome b_{559} (Cyt b_{559}) and the PsbI protein and contains six chlorophyll (Chl) and two pheophytin (Pheo) molecules. Four Chl and two Pheo in the RC are arranged in pseudo-C_2-symmetrical fashion around a non-heme iron and constitute the presumed active and inactive electron transfer branches. Two additional RC Chls, Chl_Z(D1) and Chl_Z(D2), are located at the periphery of the RC. The light harvesting capacity of the RC of PSII is increased by the association of two core antenna Chl–protein complexes, CP43 and CP47. The core complex of PSII contains about 35 Chl per RC.

Charge separation in the RC follows excitation of PSII and arises from electron transfer from the primary electron donor (P680) to Pheo creating the primary radical pair, $P680^+$/$Pheo^-$. $P680^+$ is reduced by a tyrosine radical that subsequently oxidizes the Mn cluster of the oxygen-evolving complex. When electron transport from the oxygen-evolving complex is impaired, alternative electron donors are oxidized by $P680^+$. Illumination of PSII at low temperature results in oxidation of Cyt b_{559}, or a Chl molecule if Cyt b_{559} is already oxidized [2]. It was proposed that this oxidizable Chl molecule and Cyt b_{559} form part of a low quantum yield photoprotective electron transport pathway in PSII [3]. The oxidized Chl was termed Chl_Z and subsequently identified as one of the two peripheral RC Chl molecules, Chl_Z(D1) [4]. Chl_Z appears to form part of a Cyt b_{559}-mediated cyclic electron transport pathway around PSII as it is ultimately oxidized by $P680^+$ and reduced by Cyt b_{559} which in turn is reduced by plastoquinone [5].

The presence of fractional amounts of Chl_Z^+ per RC has been correlated with a dramatic quenching of fluorescence emission from PSII [6,7]. As a strong quencher of excitation energy, Chl_Z^+ may serve a photoprotective role when the donor side of PSII is impaired.

Illumination of PSII at low temperature or in the presence of inhibitors of the oxidizing side of PSII results in the formation of an oxidized carotenoid (Car^+) as well as Chl_Z^+ [8,9]. The amounts of Chl_Z^+ and Car^+ accumulated have been shown to vary with temperature and between PSII preparations isolated from cyanobacteria and spinach [10]. It has been proposed that this Car participates in the alternative electron transfer pathway involving $P680^+$, Chl_Z and Cyt b_{559} [11]. The relative involvements and possibilities of linear, branched or parallel pathways involving Cyt b_{559}, Chl_Z and Car in electron donation to $P680^+$ have been discussed [10–13].

In cyanobacteria, the 'quenching' Chl_Z was identified, by a combination of site-directed mutagenesis and resonance Raman spectroscopy, as Chl_Z(D1) liganded to D1-His118 [4]. When the X-ray structure of PSII from *Synechococcus elongatus* was resolved [14] one surprise was that Cyt b_{559} was located on the D2 side of the PSII complex, too far from Chl_Z(D1) to reduce it directly. Interestingly, in *Chlamydomonas reinhardtii*, analogous site-directed mutations of histidines liganded to both Chl_Z(D1) and Chl_Z(D2) led to the conclu-

*Corresponding author. Fax: (1)-905-688 1855.
E-mail address: dbruce@brocku.ca (D. Bruce).

Abbreviations: PS, photosystem; Chl, chlorophyll; P680, primary electron donor for photosystem II; Chl_Z(D1) and Chl_Z(D2), peripheral reaction center chlorophylls of photosystem II; Chl_{D2}, reaction center chlorophyll of photosystem II

0014-5793/03/$22.00 © 2003 Published by Elsevier Science B.V. on behalf of the Federation of European Biochemical Societies.
doi:10.1016/S0014-5793(03)00442-3

sion that Chl_Z^+(D2) was the quenching species [15], a result more consistent with the location of Cyt b_{559}. However, another surprise from the X-ray structure was the relatively isolated location of both Chl_Z(D1) and Chl_Z(D2) from other RC chromophores and the antenna Chl of CP43 and CP47. Preliminary energy transfer calculations based on the X-ray structure showed that Chl_Z(D1) and Chl_Z(D2) were the two most weakly excitonically coupled pigments in PSII, neither would serve well as an energy quencher [16].

The X-ray structure of PSII from *Thermosynechococcus vulcanus* includes two β-carotenes [17]. The two β-carotenes are located on the D2 side of the RC near Cyt b_{559} and the RC Chl_{D2}, consistent with a role mediating electron transport between them. The involvement of Chl_Z(D1) and/or Chl_Z(D2) still remains difficult to see, as both are distant from P680, the carotenoids or Cyt b_{559}. However, the *T. vulcanus* structure contains an 'extra' Chl in CP43 located between Chl_Z(D1) and the antenna Chl of CP43. Could this Chl facilitate excitation energy transfer and electron transport between Chl_Z(D1) and the rest of PSII?

We use energy transfer models for PSII, based on the X-ray structures from *S. elongatus* and *T. vulcanus*, to calculate the quenching efficiency of a Chl cation located at a number of different sites, including Chl_Z(D1) and Chl_Z(D2). We propose a mechanism for electron transport from Chl_Z(D1) to $P680^+$ which is dependent on the location of the β-carotenes and the 'extra' Chl in CP43 found in the *T. vulcanus* structure. We suggest that a 'chain' of Chl molecules in CP43 are involved in hole migration from $P680^+$ to Chl_Z(D1) and that the quenching Chl^+ is actually an equilibrium mixture of a number of CP43 antenna Chl and Chl_Z(D1).

2. Materials and methods

Kinetic models for excitation energy transfer between all pigments in PSII were constructed based on the X-ray structures of *S. elongatus* [14,16] and *T. vulcanus* [17]. Calculation of the pairwise energy transfer rates was based on Förster theory and modified compared to our previous work [16]. For calculation of spectral overlap integrals we used absorption spectra of Chl *a* as they were determined in light harvesting complex (LHC) CP29 [18]. To calculate spectral overlap integrals for pairs with oxidized Chl_Z we used the absorption spectrum of the Chl *a* cation in butyl chloride [19] and a molar extinction at 830 nm of 8400 M^{-1} cm^{-1}. In situ dipole strengths of Chl *a* and the Chl *a* cation were extracted from the absorption spectra in medium of refractive index *n* as described in [20]. The absorption peak of the Chl_Z cation was set to 817 nm [10,11]. The shift of the emission peak relative to the absorption maximum was calculated using the universal Kennard–Stepanov relation as done previously [16]. To account for connectivity between PSII complexes, energy transfer and trapping simulations were performed with PSII core dimer structures. We introduced one Chl *a* cation per core dimer (one Chl^+ per two RCs) in the simulation and fluorescence yield was compared to the yield of the same model without the cation. Maximum fluorescence yield was calculated with the rate of charge separation set to zero to facilitate comparison with the experimentally determined quenching by photoaccumulated Chl_Z^+ in frozen PSII RCs [6,7]. Unimolecular decay rates were 0.5 ns^{-1}, the index of refraction was 1.5 [21]. The Chl cation was assumed to be a very efficient quencher and was represented by a unimolecular decay rate of 1000 ns^{-1}. Other model parameters were the same as described previously [16].

3. Results and discussion

3.1. Kinetic modeling of quenching of excitation energy by Chl^+ in PSII

To simulate Chl^+ quenching, we applied detailed kinetic models for excited state dynamics in PSII based on the X-ray structures of *S. elongatus* and *T. vulcanus*. The models were used to calculate the fluorescence yield of RCs in the absence and presence of a Chl^+ as a function of its location in PSII.

Our calculations are summarized in Table 1. Locating the Chl^+ on either Chl_Z(D1) or Chl_Z(D2) in the model based on the structure of *S. elongatus* results in much less quenching of fluorescence than on any other Chl. The quenching of approximately 30% of fluorescence in the presence of 0.5 Chl_Z^+ per RC for either Chl_Z(D1) or Chl_Z(D2) is much lower than the experimentally reported quenching of 70% of fluorescence at 0.17 Chl_Z^+ per RC at 200 K [6] or approximately 80% of fluorescence at 0.6 Chl_Z^+ per RC at 85 K [7]. The low degree of quenching is consistent with the poor energetic coupling of both Chl_Z(D1) and Chl_Z(D2) to RC and antenna pigments observed in the *S. elongatus* X-ray structure [16].

In stark contrast to Chl_Z(D1) and Chl_Z(D2), placing the Chl^+ on any other Chl in CP43 or CP47 in the model for *S. elongatus* results in much higher quenching. Most locations predict an excess of 80% quenching in the presence of the cation (Table 1).

The X-ray structure of *T. vulcanus* is similar to that of *S. elongatus*. However, one difference is the presence of an 'extra' chlorophyll in *T. vulcanus* located at the periphery of CP43 very close to Chl_Z(D1) (see Fig. 1). This Chl molecule is likely to increase the energetic coupling of Chl_Z(D1) to the antenna Chl in CP43, but by how much? In our model based on the *T. vulcanus* structure, placing the Chl^+ on Chl_Z(D1) results in much higher quenching (70%) than observed in the *S. elongatus* model. Some increased quenching was observed with the cation on Chl_Z(D2) but not nearly as much as for

Table 1
Relative fluorescence yield of PSII RCs predicted by kinetic models based on the X-ray structure of *S. elongatus* and *T. vulcanus*

Polypeptide	*S. elongatus*		*T. vulcanus*	
	Chl^+ location, CLA# in 1ILX	Rel. fluorescence	Chl^+ location, CLA# in 1IZL	Rel. fluorescence
CP43	24	0.27	17	0.26
CP43	30	0.17	23	0.18
CP43	33	0.18	26	0.15
CP47	43	0.15	36	0.18
CP47	42	0.17	35	0.21
D2, Chl_Z	20	0.67	13	0.57
D1, Chl_Z	19	0.73	12	0.30

Fluorescence yield is shown in the presence of one Chl^+ per PSII core dimer (0.5 Chl^+ per PSII RC) as a function of the location of the cation. Fluorescence yield is normalized to 1.0 in the absence of a cation. For the *S. elongatus* model, the CLA# refers to the Chl numbers in the PDB file 1ILX submitted with [16]. For the *T. vulcanus* structure the CLA# refer to the Chl numbers in the PDB file 1IZL submitted with [17]. See Section 2 for further details.

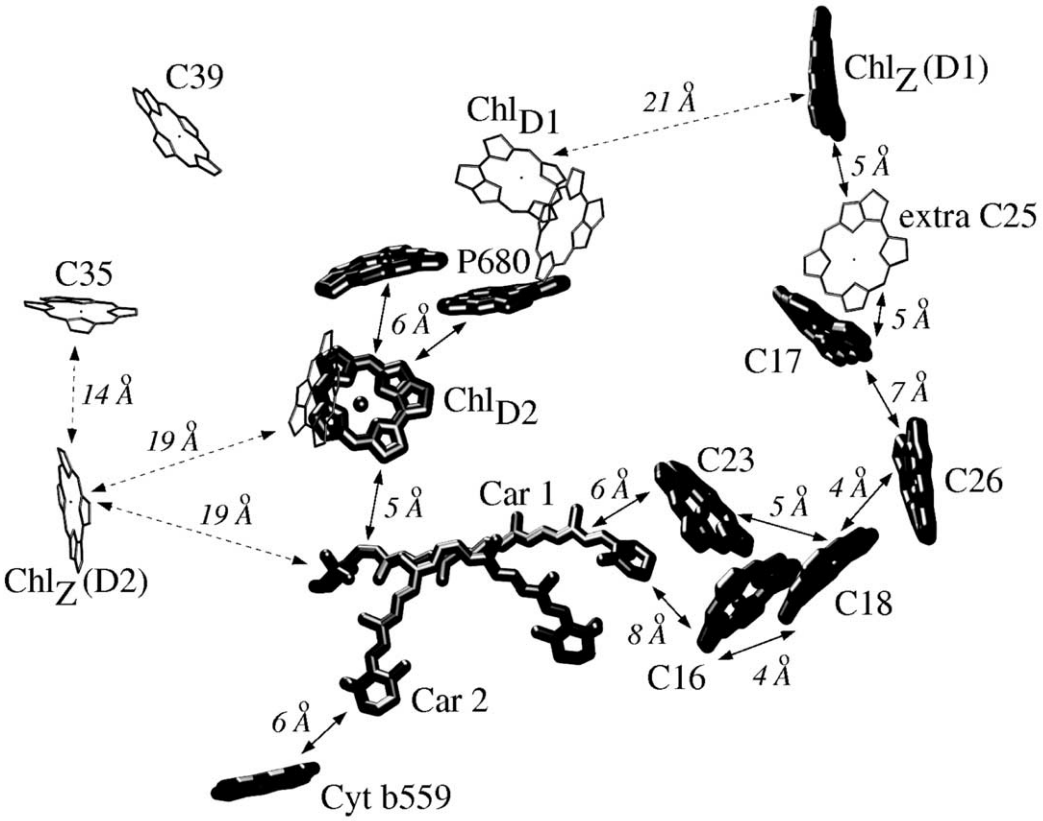

Fig. 1. Detail from the X-ray structure of *T. vulcanus* showing locations of chromophores, including the two carotenoids, the 'extra' Chl and Cyt b_{559}. Edge to edge distances between chromophores are shown in Å. The six RC Chls are identified by name, the P680 dimer, Chl_{D2}, Chl_{D1}, Chl_Z(D1) and Chl_Z(D2). Antenna Chls in CP43 and CP47 are numbered as in the PDB file 1IZL. The 'extra' Chl found in the *T. vulcanus* structure but not in the *S. elongatus* structure is labeled as 'extra' C25. The two carotenes are labeled as Car 1 and Car 2. The two ends of Car 2 were not resolved in the X-ray structure of *T. vulcanus* and one possible configuration for the complete molecule is shown in this figure.

Chl_Z(D1). Both models predict similar quenching with the cation located on other Chls in CP43 and CP47. Clearly the biggest difference between the models was the increased fluorescence quenching of Chl_Z^+(D1) predicted by the *T. vulcanus* structure as a result of increased coupling due to the 'extra' Chl.

3.2. *A mechanism for the oxidation of Chl_Z(D1) involving β-carotene and a number of CP43 antenna Chls. A novel electron transport pathway*

The *T. vulcanus* X-ray structure of PSII locates one of the β-carotenes (Car 1) close to the RC Chl_{D2} (8 Å) and to Chls C23 and C16 of CP43, (6 Å and 8 Å, respectively) (Fig. 1). These Chl form part of a chain of Chl molecules in CP43 (C18, C26, C17), all within 7 Å of each other, which lead to the 'extra' Chl of CP43 (C25). This 'extra' Chl completes the chain of closely spaced molecules leading from the RC to Chl_Z(D1). The other β-carotene (Car 2) is in close contact with Car 1 and within 6 Å of the heme of Cyt b_{559}.

We suggest that this chain of pigments offers a pathway for electron transport between Chl_Z(D1) and $P680^+$ and Cyt b_{559}. Edge to edge distances between the chromophores in this chain are all less than 8 Å. An estimate of the rate of electron transfer at such a distance, based on the empirical expression of Dutton [22], is about 25 ns^{-1}. In contrast, the calculated transfer rate between Chl_Z(D2) and RC pigments and/or carotenoids (the closest distance is 19 Å) is 6.3×10^{-6} ns^{-1}. We suggest that in cyanobacteria, identification of Chl_Z(D1) as the quenching cation [4] may be explained by migration of the electron hole from $P680^+$ through Chl_{D2}, the carotenoid and a chain of antenna Chl in CP43 to Chl_Z(D1).

The relative accumulation of oxidized Car and Chl induced by illumination at low temperature in the presence of oxidized Cyt b_{559} is temperature-, species- and preparation-dependent [10]. The most recent interpretations of optical spectra suggest the presence of a number of different Chl^+ in samples illuminated at low temperature (C. Tracewell and G. Brudvig, in preparation). These results are consistent with the idea of a chain of CP43 antenna Chl forming an electron transport pathway between $P680^+$ and Chl_Z(D1). The distribution of the hole between the pigments involved in this chain will be defined by their relative reduction potentials. The experimentally observed distribution of the cation between a number of Chl^+ species is consistent with the idea that the relative reduction potentials of these molecules may vary in samples where individual RCs have been frozen into slightly different conformations. The preferential formation of Chl_Z^+(D1) may reflect a somewhat higher dielectric environment for this pigment, possibly resulting from its peripheral position. However, as seen in Table 1, the location of the cation does not greatly affect its relative quenching ability and we suggest that under physiological temperatures the quenching Chl^+ in cyanobacteria is distributed over a number of CP43 antenna Chl and Chl_Z(D1).

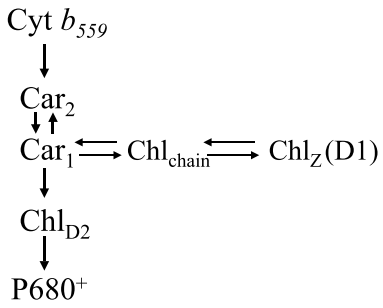

Fig. 2. Alternative electron transport scheme based on the distances between cofactors found in the *T. vulcanus* X-ray structure. See text for details.

The potential electron transport pathway between Cyt b_{559}, $Chl_Z(D1)$ and $P680^+$ involving the two carotenoids and a series of CP43 antenna Chl inferred from the structure of PSII in *T. vulcanus* is shown in Fig. 2. The structure immediately suggests a branched pathway where either Cyt b_{559} or $Chl_Z(D1)$ may donate electrons to $P680^+$ when the donor side of PSII is impaired. This is consistent with an earlier proposal of a branched pathway for Cyt b_{559} and $Chl_Z(D1)$ involving a Car^+ [11] and the position of the Car within this pathway is consistent with [10]. We propose that when Cyt b_{559} is reduced, electron transport from Cyt b_{559} to Car 2 to Car 1 to Chl_{D2} to $P680^+$ is the predominant pathway. When Cyt b_{559} is oxidized, the pathway would be from $Chl_Z(D1)$ through the chain of CP43 antenna Chl to Car 1 to Chl_{D2} to $P680^+$. This scheme also allows for the reduction of $Chl_Z(D1)^+$ by reduced Cyt b_{559}. The redox state of Cyt b_{559} thus remains the control point for both the formation and loss of the quenching Chl cation.

Our hypothesis is supported by model simulations and is consistent with experimental data acquired for cyanobacterial PSII. The role of $Chl_Z(D1)$ in this hypothesis is, however, dependent on the position of the 'extra' Chl in CP43, C25 in Fig. 1, which is observed only in the *T. vulcanus* structure. Chl C25 is responsible for completing the proposed electron transport pathways between Cyt b_{559}, P680 and $Chl_Z(D1)$ and for increasing the energetic coupling of $Chl_Z(D1)$ to other PSII Chl. However, even in the absence of C25 our hypothesis still predicts the involvement of multiple Chl^+, and locates them in CP43. The positions of Chls in the *T. vulcanus* structure are very similar to those in the *S. elongatus* structure, with two exceptions. In CP47 one additional Chl was found in *T. vulcanus* that was not present in *S. elongatus*. This Chl, CLA43 in PDB file 1IZL, is located in a relatively peripheral location and its presence does not change our modeling results. In CP43, *T. vulcanus* shows one 'extra' Chl (CLA25 in PDB file 1IZL) and one 'missing' Chl (CLA33 in PDB file 1ILX) when compared to *S. elongatus*. Both of the Chls observed in *T. vulcanus* but not in *S. elongatus* were found in relatively peripheral positions. Although this may reflect structural differences between the two species it is possible that these Chls were lost in the isolation of PSII from *S. elongatus* but retained in *T. vulcanus*.

3.3. Identification of the quenching Chl_Z^+ in higher plants

Quenching may be different in higher plant PSII. In *C. reinhardtii* site-directed mutants of the $Chl_Z(D2)$ ligand decreased the magnitude of illumination-induced fluorescence quenching associated with Chl^+ formation at 200 K (by about 20%) while mutation of the $Chl_Z(D1)$ ligand did not [15]. In addition, the lineshape of the X-band electron paramagnetic resonance (EPR) signal attributed to Chl_Z^+ was broadened in the D2 mutant but not in the D1 mutant. However, mutations which affect the activity of the RC and/or energetic coupling of antenna could also affect the relative yield of chlorophyll cation and/or fluorescence yield. In addition, the change in lineshape of the EPR signal is consistent with an increase in the relative contribution of Car^+ to the signal, as shown in [4,11]. It is difficult to positively identify the cation by the X-band EPR signal. Optical spectra have shown the presence of a number of different Chl^+ and a Car^+ in *Chlamydomonas* [10] that contribute to the EPR signal associated with Chl_Z^+. Comparisons of structural data for the higher plant LHCII–PSII supercomplex and cyanobacterial PSII core complex have pointed out differences in the membrane-spanning helices near both $Chl_Z(D1)$ and $Chl_Z(D2)$ [23]. This structural variation may account for the observed differences in amount and species of cation accumulated in *Chlamydomonas* and cyanobacteria [10]. At present, it is not possible to tell if the mechanism for quenching by $Chl_Z^+(D1)$ we have proposed, based on the *T. vulcanus* structure, is applicable to higher plants. However, the presence of multiple Chl^+ in *Chlamydomonas* is consistent with our hypothesis.

Acknowledgements: We thank J.-R. Shen and N. Kamiya for early access to their X-ray structure for PSII from *Thermosynechococcus vulcanus*. D.B. is supported by the Natural Sciences and Engineering Research Council of Canada. G.W.B. is supported by the U.S. Department of Energy, Office of Basic Energy Sciences, under Contract DE-F-G02-01ER15281.

References

[1] Niyogi, K.K. (1999) Annu. Rev. Plant Physiol. Plant Mol. Biol. 50, 333–359.
[2] de Paula, J.C., Innes, J.B. and Brudvig, G.W. (1985) Biochemistry 24, 8114–8120.
[3] Thompson, L.K. and Brudvig, G.W. (1988) Biochemistry 27, 6653–6658.
[4] Stewart, D.H., Cua, A., Chisholm, D.A., Diner, B., Bocian, D.F. and Brudvig, G.W. (1998) Biochemistry 37, 10040–10046.
[5] Stewart, D.H. and Brudvig, G.W. (1998) Biochim. Biophys. Acta 1367, 63–87.
[6] Schweitzer, R.H. and Brudvig, G.W. (1997) Biochemistry 36, 11351–11359.
[7] Schweitzer, R.H., Melkozernov, A.N., Blankenship, R.E. and Brudvig, G.W. (1998) J. Phys. Chem. B 102, 8320–8326.
[8] Schenck, C.C., Diner, B., Mathis, P. and Satoh, K. (1982) Biochim. Biophys. Acta 680, 216–227.
[9] Mathis, P. and Rutherford, A.W. (1984) Biochim. Biophys. Acta 767, 217–222.
[10] Tracewell, C.A., Cua, A., Stewart, D.H., Bocian, D.F. and Brudvig, G.W. (2001) Biochemistry 40, 193–203.
[11] Hanley, J., Deligiannakis, Y., Pascal, A., Faller, P. and Rutherford, A.W. (1999) Biochemistry 38, 8189–8195.
[12] Faller, P., Pascal, A. and Rutherford, A.W. (2001) Biochemistry 40, 6431–6440.
[13] Tracewell, C.A., Vrettos, J.S., Bautista, J.A., Frank, H.A. and Brudvig, G.W. (2001) Arch. Biochem. Biophys. 385, 61–69.
[14] Zouni, A., Witt, H.-T., Kern, J., Fromme, P., Krauß, N., Saenger, W. and Orth, P. (2001) Nature 409, 739–743.
[15] Wang, J., Gosztola, D., Ruffle, S.V., Hemann, C., Seibert, M., Wasielewski, M.R., Hille, R., Gustafson, T.L. and Sayre, R.T. (2002) Proc. Natl. Acad. Sci. USA 99, 4091–4096.
[16] Vasil'ev, S., Orth, P., Zouni, A., Owens, T.G. and Bruce, D. (2001) Proc. Natl. Acad. Sci. USA 98, 8602–8607.

[17] Kamiya, N. and Shen, J.R. (2003) Proc. Natl. Acad. Sci. USA 100, 98–103.
[18] Cinque, G.R., Croce, R. and Bassi, R. (2000) Photosynth. Res. 64, 233–242.
[19] Hoshino, M., Ikehara, K., Imamura, M., Seki, H. and Hama, Y. (1981) Photochem. Photobiol. 34, 75–81.
[20] Knox, R.S. and van Amerongen, H. (2002) J. Phys. Chem. B 106, 5289–5293.
[21] Gruszecki, W.I., Grudzinski, W., Banaszek-Glos, A., Matula, M., Kernen, P., Krupa, Z. and Sielewiesiuk, J. (1999) Biochim. Biophys. Acta 1412, 173–183.
[22] Moser, C.C., Keske, J.M., Warncke, K., Farid, R.S. and Dutton, P.L. (1992) Nature 355, 796–802.
[23] Tracewell, C.A. and Brudvig, G.W. (2002) in: Proceedings. 12th International Congress on Photosynthesis, CSIRO, Canberra, http://www.publish.csiro.au/PS2001.